THE JOURNAL OF PHYSICAL CHEMISTRY A

Article

Cite This: J. Phys. Chem. A 2019, 123, 999−1006

pubs.acs.org/JPCA

# Kinetics of the Methyl−Vinyl Radical + $O_2$ Reactions Associated with Propene Oxidation

Satya P. Joshi,[§] Timo T. Pekkanen,[§] Raimo S. Timonen,[§] György Lendvay,[#] and Arkke J. Eskola*[,§]

[§]Department of Chemistry, University of Helsinki, P.O. Box 55 (A.I. Virtasen aukio 1), FI-00014, Helsinki, Finland

[#]Institute of Materials and Environmental Chemistry, Research Centre for Natural Sciences, Hungarian Academy of Sciences, Magyar tudósok krt. 2, Budapest, H-1117, Hungary

Supporting Information

**ABSTRACT:** The bimolecular rate coefficients of reactions $CH_3CCH_2$ + $O_2$ (1) and *cis/trans*-$CH_3CHCH$ + $O_2$ (2a/3a) have been measured using a tubular laminar flow reactor coupled with a photoionization mass spectrometer (PIMS). These reactions are relevant in the combustion of propene. Pulsed excimer laser photolysis of a ketone or a bromide precursor molecule at 193 or 248 nm wavelength was used to produce radicals of interest homogeneously along the reactor. Time-resolved experiments were performed under pseudo-first-order conditions at low pressure (0.3−1.5 Torr) over the temperature range 220−660 K. The measured bimolecular rate coefficients were found to be independent of bath gas concentration. The bimolecular rate coefficients possess negative temperature dependence at low temperatures ($T$ < 420 K) and appear to be independent of temperature at high temperatures ($T$ > 420 K). Observed products of the reaction $CH_3CCH_2$ + $O_2$ were $CH_3$ and $H_2CO$, while for the reaction *cis/trans*-$CH_3CHCH$ + $O_2$, observed products were $CH_3CHO$ and HCO. Current results indicate that the reaction mechanism of both reactions is analogous to that of $C_2H_3$ + $O_2$. Methyl substitution of the vinyl radical changes its reactivity toward $O_2$ upward by ca. 50% if it involves the $\alpha$-position and downward by ca. 30% if the methyl group takes either of the $\beta$-positions, respectively.

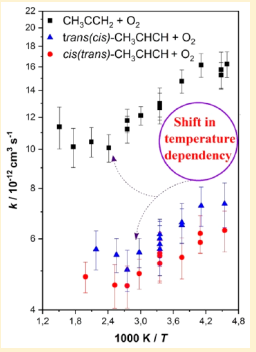


## INTRODUCTION

Propene is the second simplest unsaturated hydrocarbon after ethene and serves as a key compound in the petrochemical industry. Propene is also an important intermediate species in the combustion of propane and larger hydrocarbons and has a significant impact on combustion processes.[1−5] The presence of a double bond in the propene molecule gives it a relatively high thermal stability. Abstraction of the weakest H atom from propene molecule produces a resonance-stabilized allyl radical, which is highly stable against unimolecular decomposition. The allyl radical reacts very slowly with $O_2$ and can thus reach high concentrations under high temperature conditions. Consequently, the allyl radical is an important precursor in the formation of aromatic structures which may fuse together and finally lead to the soot formation.[6−8] As shown in Scheme 1, four different radicals can be produced from propene via hydrogen abstraction reactions. Three of the four radicals ($CH_3CCH_2$, *cis*-$CH_3CHCH$, and *trans*-$CH_3CHCH$) are vinyl-type and $CH_2CHCH_2$ is the resonance stabilized allyl radical.

Considering that the bond dissociation energy (BDE, $D_0$) of vinylic hydrogens is ∼94 kJ/mol higher than that of the allylic hydrogens of propene[9−11] it is obvious that allyl radicals are produced in significantly higher abundance than methyl−vinyl radicals. Burke et al.[12] performed a reaction flux analysis of the propene oxidation experiments conducted in a jet-stirred-reactor (JSR) and showed that in a mixture of 1.67% propene and 3.38% $O_2$ in helium ($T$ = 970 K, equivalence ratio $\phi$ = 2.19), oxidation resulted in 54% formation of allylic radical and only 9% formation of the combined other three methyl−vinyl radicals. While they are formed with a relatively low abundance, methyl−vinyl radicals are highly reactive in comparison to the very unreactive allyl radical. If one considers specifically the kinetics of the methyl−vinyl + $O_2$ reactions, their impact on combustion chemistry turns out to be rather important and needs to be included in accurate combustion chemistry models. The Burke et al.[12] reaction flux analysis of

**Scheme 1. Production of Methyl−Vinyl and Allyl Radicals from Propene via Hydrogen Abstraction Reactions**[a]

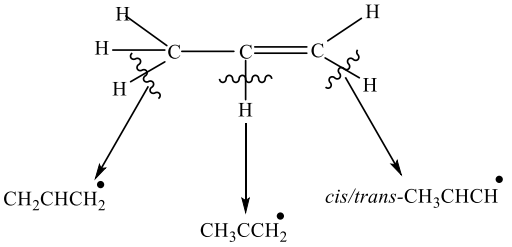


[a]The C−H bond dissociation energies associated with the formation of allyl radical $CH_2CHCH_2$, methyl-vinyl radicals $CH_3CCH_2$, *trans*-$CH_3CHCH$, and *cis*-$CH_3CHCH$ are 360.7 kJ mol$^{-1}$, 443.9 kJ mol$^{-1}$, 461.1 kJ mol$^{-1}$, and 459.0 kJ mol$^{-1}$, respectively.[9−11]

**Received:** November 13, 2018
**Revised:** December 28, 2018
**Published:** January 4, 2019

propene oxidation also showed that 47% of the $CH_2CHCH_2$ radicals produced were consumed by the $CH_2CHCH_2 + HO_2$ reaction and only 14% were consumed by the $CH_2CHCH_2 + O_2$ reaction. Under the same conditions, however, almost all of the methyl−vinyl radicals produced were consumed via reaction with $O_2$.[12]

Slagle et al.[13] carried out an experimental kinetic study of the $CH_3CHCH + O_2$ reaction employing the laser photolysis−photoionization mass spectrometry (PIMS) method to produce and detect $CH_3CHCH$ radicals. The bimolecular reaction rate coefficient was measured over the temperature range 296−600 K, and no dependence on temperature or bath gas concentration (pressure) was observed. However, a recent theoretical and computational study of *trans*-$CH_3CHCH + O_2$ reaction by Chen and Goldsmith[14] show an explicit temperature dependence. Slagle et al.[13] did not report whether they were investigating a single isomer or a mixture of both isomers (*cis*-$CH_3CHCH$ or/and *trans*-$CH_3CHCH$).

The purpose of the present work is to perform direct kinetic experiments of reactions 1−3 individually:

$$CH_3CCH_2 + O_2 \rightarrow \text{products} \quad (1)$$

$$cis\text{-}CH_3CHCH + O_2 \rightarrow \text{products} \quad (2)$$

$$trans\text{-}CH_3CHCH + O_2 \rightarrow \text{products} \quad (3)$$

The aim is to better understand the temperature dependence of the bimolecular rate coefficients of these oxidation reactions and compare the experimental results with the computational results of Chen and Goldsmith,[14] who combined high level ab initio calculations with master equation modeling to study the kinetics of reactions 1 and 3. To our knowledge, there are no previous measurements available on the $CH_3CCH_2 + O_2$ reaction. The reaction of vinyl radical, $CH_2CH + O_2$, has key importance in the modeling of combustion processes and has been studied extensively.[15−22] The current study also aims to quantify the effect of an H atom substitution in vinyl radical by a methyl group on the oxidation kinetics.

## EXPERIMENTAL SECTION

Pulsed excimer laser photolysis of a relevant precursor molecule was used to produce the radical of interest, and its decay was followed in real-time using a PIMS for which ionizing radiation was provided by a microwave-powered gas-discharge lamp. The experimental apparatus and procedures employed have already been described previously,[22] hence only a brief description of experimental details specific to this work are presented in this section.

The reaction gas mixture flowing through the temperature controlled tubular reactor contained mostly the inert helium bath-gas (>99%) and molecular oxygen. The mixture contained a relatively small amount of precursor (<0.03%), which was introduced into the reactor by constantly bubbling helium through a temperature-controlled precursor cavity. The gas mixture containing the precursor was photolyzed using 193 nm (ArF) or 248 nm (KrF) radiation from an exciplex laser (ASX-750) along a reactor axis to achieve a homogeneous concentration of radicals along the reactor. All measurements were done under pseudo-first-order conditions, that is, $[R]/[O_2] \leq 0.05$. For the production of methyl−vinyl radicals, the following precursors were used:

3-Methyl-3-buten-2-one precursor was used to produce $CH_3CCH_2$ radicals:

$$CH_3C(O)C(CH_3)CH_2 + h\nu\ (193\ nm) \rightarrow CH_3CCH_2 + CH_3CO$$
$$\rightarrow CH_3CCH_2 + CH_3 + CO$$
$$\rightarrow \text{other products} \quad (P1a)$$

Since $CH_3CO$ can further undergo chemically activated decomposition to give CO and $CH_3$, and methyl radical is one potential product of the reaction $CH_3CCH_2 + O_2$, another precursor, 2-bromopropene, was used in product detection measurements.

$$CH_3C(Br)CH_2 + h\nu\ (193\ nm) \rightarrow CH_3CCH_2 + Br$$
$$\rightarrow \text{other products} \quad (P1b)$$

For generating the $CH_3CHCH$ radical, which has a *cis*- and a *trans*-isomer, the corresponding bromides were employed:

$$cis\text{-}CH_3CHCHBr + h\nu\ (193/248\ nm) \rightarrow cis/trans\text{-}CH_3CHCH + Br$$
$$\rightarrow \text{other products} \quad (P2a)$$

$$trans\text{-}CH_3CHCHBr + h\nu\ (193/248\ nm) \rightarrow trans/cis\text{-}CH_3CHCH + Br$$
$$\rightarrow \text{other products} \quad (P2b)$$

As shown in Figure 1, the isomerization barrier separating the *cis*-$CH_3CHCH$ and *trans*-$CH_3CHCH$ isomers is very small (<20 kJ/mol) and can be easily surpassed even if the newly formed methyl−vinyl radical loses some part of the excess energy (>140 kJ/mol) available after laser photolysis at 193 or 248 nm. Hence it is possible that although we have used *cis*-1-bromopropene and *trans*-1-bromopropene to produce *cis*-$CH_3CHCH$ and *trans*-$CH_3CHCH$ radicals, respectively, both these radicals may have isomerized to each other to some extent before being thermalized by collisions with the buffer gas molecules. Consequently, photolyzing isomerically pure precursors at either wavelength may lead to an isomeric mixture of *cis*-$CH_3CHCH$ and *trans*-$CH_3CHCH$. The fact that we observed different decay rates depending on which precursor isomer was used indicates that equilibration of the two radical isomers was not achieved. Hereafter, the following notation is used to take this into account: reactions 2a and 3a represent the conditions in which radicals were produced using *cis*-1-bromopropene and *trans*-1-bromopropene precursors, respectively, and isomerization took place to an unknown extent.

$$cis(trans)\text{-}CH_3CHCH + O_2 \rightarrow \text{products} \quad (2a)$$

$$trans(cis)\text{-}CH_3CHCH + O_2 \rightarrow \text{products} \quad (3a)$$

The measurements were carried out under low pressure (0.3−1.5 Torr) conditions using a quartz or stainless steel reactor that had an inner diameter of 17 mm. The flow velocity in the reactor was maintained at about 5 $ms^{-1}$ in order to ensure that the gas-mixture was completely replaced between laser pulses with the employed repetition rate of 5 Hz. The reactor tube employed was either uncoated or coated with halocarbon wax or polydimethylsiloxane. The reaction mixture was continuously sampled via a 0.4 mm diameter hole on the reactor wall forming a beam expanding into high-vacuum. A conical skimmer selected the center portion of the beam, producing a collimated beam before it entered the ionization chamber



DOI: 10.1021/acs.jpca.8b11017
J. Phys. Chem. A 2019, 123, 999−1006

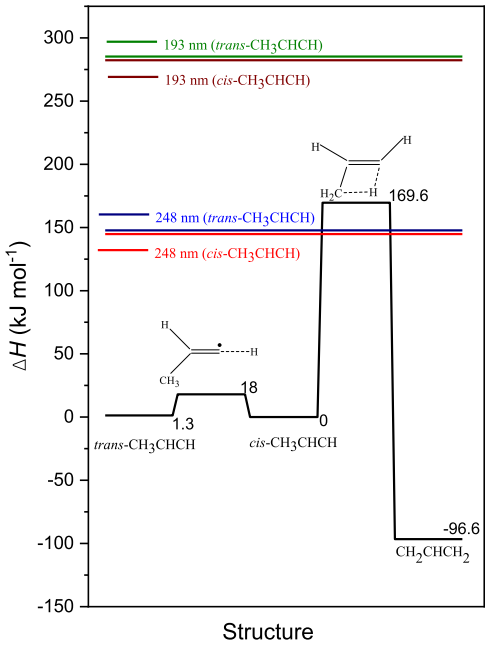


**Figure 1.** Relative enthalpies at 298 K of the *trans*- and *cis*-methylvinyl isomers and allyl radical along with the isomerization saddle points in kJ/mol, calculated at the CCSD(T)/cc-pVTZ//CCSD/cc-pVTZ level using the CCSD/cc-pVDZ//CCSD/cc-pVDZ vibrational frequencies. The details of electronic structure calculations are described in the Supporting Information, and Figure S1 shows calculated bond distances for the H atom shift in the transition structure associated with *cis*-$CH_3CHCH$ ↔ $CH_2CHCH_2$ isomerization. The colored horizontal lines represent the maximum energy available for the isomerization of the nascent *cis*-$CH_3CHCH$ and *trans*-$CH_3CHCH$ radicals produced by the photolysis of *cis*-1-bromopropene and *trans*-1-bromopropene at 193 and 248 nm, respectively, and were calculated by subtracting the bond dissociation energy (BDE) of C−Br bond [BDE(*cis*-1-bromopropene) = 337.6 kJ $mol^{-1}$ and BDE(*trans*-1-bromopropene) = 334.7 kJ $mol^{-1}$][23] from the energy of the 193 and 248 nm photon, assuming that the accompanying Br-atom is formed in the ground state.

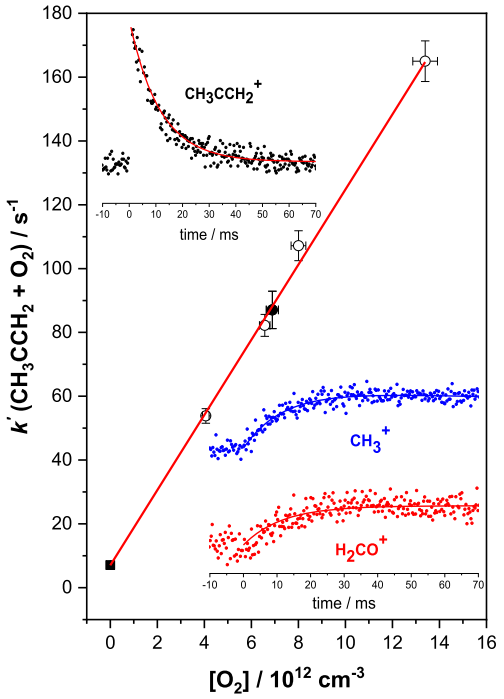


**Figure 2.** A bimolecular plot for the $CH_3CCH_2$ + $O_2$ reaction measured at $T$ = 363 K and $p$ = 0.73 Torr. The shown uncertainties are 1$\sigma$. On the top left corner is a typical $CH_3CCH_2$ radical decay profile with $k'_{decay}$ ($CH_3CCH_2$) = 87 ± 5.9 $s^{-1}$. On the bottom right corner are shown the observed ion signal profiles of $CH_3$ (blue) and $H_2CO$ (red), the expected reaction products.

containing the PIMS. Ionization radiation (8.9−9.1 eV) was provided by a microwave-discharge of $Cl_2$-helium mixture (Cl-lamp) with a $CaF_2$ window and was used for the detection of all three vinyl-type radicals, which have an $m/z$ value of 41 ($C_3H_5^+$). The observed reaction products were ionized with a $H_2$-lamp with a $MgF_2$ window (10.2 eV) and an Ar-lamp with a LiF window (11.6−11.8 eV). The ions produced were mass-selected by the quadrupole mass-spectrometer followed by their detection using an off-axis electron multiplier. The temporal ion signal (see insets in Figures 2 and 3) was recorded using a multichannel scaler from 10 ms before and up to 70 ms after each laser pulse and transferred to a computer for the subsequent analysis. Typically the R decay signal profile was accumulated from 3000−8000 repetitions before the nonlinear least-squares method was used to fit an exponential function, $[R_t] = A + [R_0] \times \exp(-k't)$, to the data. Here $[R_t]$ is proportional to the radical concentration at time $t$, $k'$ is the pseudo-first-order decay rate coefficient, and $A$ is the background signal.

Initial radical concentrations were kept low, at, or below about 2 × $10^{11}$ $cm^{-3}$, in order to suppress any radical−radical reactions. Under pseudo-first-order experimental conditions ($[R] \ll [O_2]$) with low initial radical concentrations, only two significant reactions, A and B, contribute to the loss rate of radical R:

$$R + O_2 \rightarrow \text{products} \quad (A)$$

$$R \xrightarrow{k_{wall}} \text{heterogeneous loss} \quad (B)$$

Reaction A is the bimolecular gas-phase reaction between R and the reactant ($O_2$) and is the primary interest in the current work. Reaction B is denoted as $k_{wall}$ and involves radical losses on the reactor wall as well as other slow first-order reactions (e.g., with radical precursor, with impurities in buffer gas, etc.) without added reactant. The first-order decay rate without added reactant, $k_{wall}$, was determined in the beginning and end of each bimolecular rate coefficient measurement. The first-order decay rate coefficient $k'$ was then measured as a function of $[O_2]$, where the fastest $k'$ obtained was typically at least 5 × $k_{wall}$. Since the only significant reactions consuming R during the experiments were reactions A and B, the bimolecular reaction rate coefficient $k(R + O_2)$ could be obtained from the slope of the $k'$ versus $[O_2]$ plot according to the equation $k' = k(R + O_2) \times [O_2] + k_{wall}$. Typical bimolecular plots to obtain $k(R + O_2)$ are shown in Figures 2 and 3.

The precursors 2-bromopropene (Sigma-Aldrich, > 99%), *cis*-1-bromopropene (Sigma-Aldrich, > 97%), *trans*-1-bromopropene (Sigma-Aldrich, > 99%), and 3-methyl-3-buten-2-one (TCI, > 95%) were degassed by several freeze−pump−thaw cycles before use. Helium (Messer-Griesheim, purity of 99.9996%) and $O_2$ (Aga, purity of 99.998%) were used as supplied. The gas pressures were monitored by capacitance pressure gauges. Estimated temperature uniformity of the reaction zone is ±2 K.



DOI: 10.1021/acs.jpca.8b11017
J. Phys. Chem. A 2019, 123, 999−1006

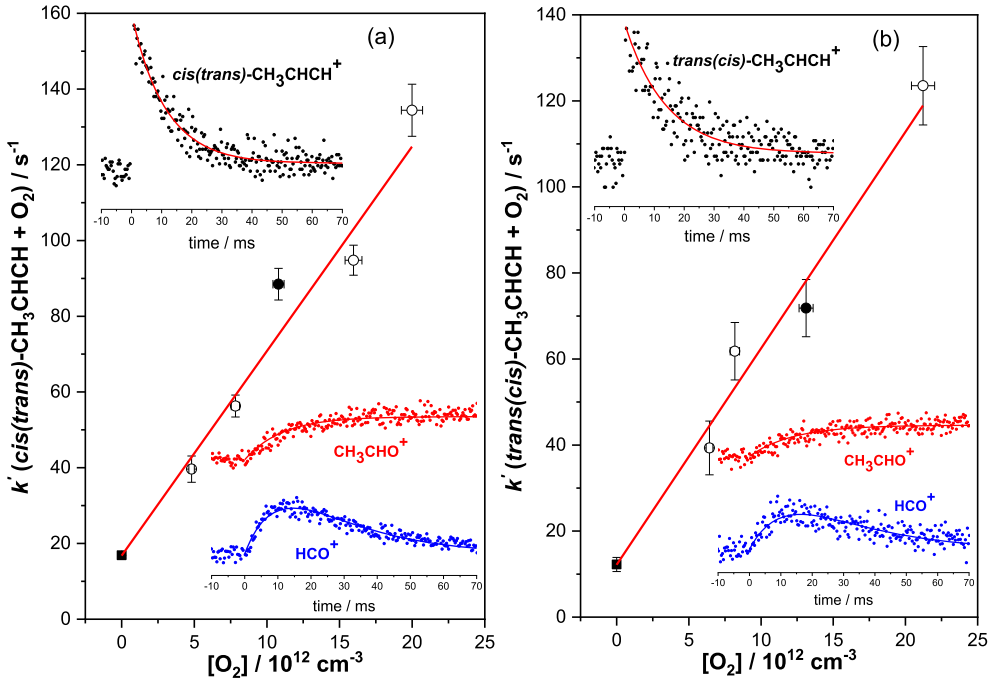


**Figure 3.** Bimolecular plots for the reactions (a) *cis*(*trans*)-$CH_3CHCH$ + $O_2$ ($T$ = 266 K, $p$ = 1.04 Torr) and (b) *trans*(*cis*)-$CH_3CHCH$ + $O_2$ ($T$ = 363 K, $p$ = 1.4 Torr) measured under pseudo-first-order conditions. The shown uncertainties are 1$\sigma$. Typical radical decay profiles for (a) *cis*(*trans*)-$CH_3CHCH$ and (b) *trans*(*cis*)-$CH_3CHCH$ are shown on the top left corner of panels a and b, respectively, with $k'$ (*cis*(*trans*)-$CH_3CHCH$) = 88.5 ± 4.2 $s^{-1}$ and $k'$ (*trans*(*cis*)-$CH_3CHCH$) = 71.8 ± 6.6 $s^{-1}$. At the bottom right corner of both panels are shown the observed ion signal profiles of $CH_3CHO$ (red) and HCO (blue), the expected reaction products.

## RESULTS AND DISCUSSION

The measured bimolecular rate coefficients of reactions 1 $CH_3CCH_2$ + $O_2$, (2a) *cis*(*trans*)-$CH_3CHCH$ + $O_2$, and (3a) *trans*(*cis*)-$CH_3CHCH$ + $O_2$ are presented in Table 1 along with the corresponding experimental conditions. The estimated uncertainty of the bimolecular rate coefficients is ±20%. This originates from uncertainties in fitting processes, in flow rate measurements, and slight temperature fluctuations (±2 K) during measurements.

The radical decay signals along with the corresponding product formation signals are shown in Figures 2 and 3. Formaldehyde ($H_2CO$, Ar/LiF) and methyl radical ($CH_3$, $H_2$/$MgF_2$) were observed as products of reaction 1. For reactions 2a and 3a, the observed products were formyl radical (HCO, $H_2$/$MgF_2$) and acetaldehyde ($CH_3CHO$, $H_2$/$MgF_2$). Assuming an analogy with the reaction $C_2H_3$ + $O_2$ → CHO + $H_2CO$, the expected products are $H_2CO$ and acetyl radical ($CH_3CO$) for reaction 1 and HCO and $CH_3CHO$ for reactions 2a and 3a. The calculations of Chen and Goldsmith[14] for reactions 1 and 3 at low pressures and temperatures support our expectations. We did not directly observe any signal for the formation of $CH_3CO$ at $m/z$ = 43 for reaction 1; we believe that the formed $CH_3CO$ underwent chemically activated decomposition to produce $CH_3$ and CO, of which $CH_3$ was observed at $m/z$ = 15. This is likely since the products of the $CH_3CCH_2$ + $O_2$ → $H_2CO$ + $CH_3CO$ reaction channel are formed with ∼90 kcal/mol (377 kJ/mol) of excess energy[14] and the threshold energy for decomposition $CH_3CO$ → $CH_3$ + CO is only about 15.6 kcal/mol (65.3 kJ/mol).[24] None of the product signals were detected in the absence of $O_2$. Hence, we conclude that under the experimental conditions of our measurements, the major product channels are the formation of $H_2CO$ and $CH_3CO$ for reaction 1 and the formation of HCO and $CH_3CHO$ for reactions 2a and 3a. The nature of the products formed for reactions 1, 2a, and 3a indicate that the reaction mechanism involves the formation of a cyclic intermediate containing an O−O bond, decomposition of which is a highly exothermic process.

The nonlinear least-squares method was used to fit the equation $I_t(P^+) = B + I_0(P^+)(1 - \exp(-k't))$ to the formation signals of the closed-shell products $CH_3CHO$ and $H_2CO$. Here parameters $B$, $I_0(P^+)$, and $k'$ are the non-time-resolved background signal, the signal value at $t \to \infty$, corresponding to channel yield × $[R_{vinyl}]_0$, and the pseudo-first-order decay rate coefficient. Since the other two products, $CH_3$ and HCO, are open-shell species and react with $O_2$, although the $CH_3$ + $O_2$ reaction is very slow ($k' \leq 0.03$ $s^{-1}$) under our experimental conditions, the following expression was fitted to the signal profiles:

$$I_t(P^+) = B + I_0(P^+)\left(\frac{k'}{k' - k'_p}\right)(\exp(-k'_p t) - \exp(-k't))$$

where $k'_p$ is a pseudo-first-order rate coefficient of the reaction of the open-shell species with $O_2$ and is treated as an individual fitting parameter.

Experiments were performed at different temperatures and pressures to determine the bath gas concentration dependence and temperature dependence of the measured bimolecular rate coefficients. No bath gas concentration dependence (pressure dependence) was observed for the rate coefficients of reactions 1−3, an observation that is in agreement with the computational results of Chen and Goldsmith[14] under low-pressure conditions of the current work. Similarly, no pressure dependence has been observed for the $C_2H_3$ + $O_2$ reaction.[15−22] Arrhenius plots of the bimolecular rate


DOI: 10.1021/acs.jpca.8b11017
J. Phys. Chem. A 2019, 123, 999−1006

**Table 1. Conditions and Results of the Experiments Used to Measure the Bimolecular Rate Coefficients of Reactions 1, 2a, and 3a**

| $T$[a] (K) | $p_{He}$ (Torr) | [He] ($cm^{-3}$) $10^{16}$ | [Pr] ($cm^{-3}$) $10^{12}$ | [$O_2$] ($cm^{-3}$) $10^{12}$ | $k'$ ($s^{-1}$) | $k_{wall}$[b] ($s^{-1}$) | $k_{wall}$[c] ($s^{-1}$) | $k$ (R + $O_2$) ($cm^3$ $s^{-1}$) $10^{-12}$ |
|---|---|---|---|---|---|---|---|---|
| | | | | $CH_3CCH_2$[d] | | | | |
| 218 | 0.44 | 1.95 | 0.91 | 2.63−7.25 | 60.4−136 | 19.7 ± 0.6 | 19.6 ± 0.8 | 16.3 ± 1.2 |
| 223 | 0.45 | 1.95 | 0.86 | 2.60−9.65 | 54.7−160 | 14.5 ± 0.5 | 14.8 ± 1.0 | 15.3 ± 1.1 |
| 223 | 0.88 | 3.79 | 1.21 | 2.53−10.2 | 61.8−165 | 13.6 ± 0.6 | 15.0 ± 2.6 | 15.8 ± 1.7 |
| 243 | 0.49 | 1.95 | 1.31 | 2.58−6.50 | 56.0−114 | 13.5 ± 0.5 | 13.6 ± 0.6 | 16.2 ± 1.1 |
| 266 | 0.54 | 1.96 | 0.97 | 2.62−10.9 | 52.3−171 | 12.5 ± 0.6 | 12.8 ± 0.6 | 14.7 ± 1.0 |
| 298 | 0.60 | 1.94 | 1.14 | 2.87−8.57 | 46.4−125 | 9.05 ± 0.8 | 8.94 ± 1.2 | 13.0 ± 1.2 |
| 298 | 1.11 | 3.60 | 1.01 | 2.58−8.49 | 38.7−129 | 530 ± 0.9 | 5.92 ± 1.1 | 123 ± 1.1 |
| 298[e] | 0.40 | 1.30 | 1.37 | 5.69−15.4 | 127−242 | 51.8 ± 0.8 | 52.1 ± 1.0 | 12.9 ± 0.9 |
| 333 | 0.68 | 1.97 | 0.88 | 3.28−11.2 | 46.4−142 | 6.94 ± 0.7 | 6.92 ± 0.1 | 12.1 ± 0.6 |
| 363 | 0.73 | 1.94 | 0.94 | 4.06−13.4 | 53.8−165 | 7.08 ± 0.7 | 7.01 ± 0.5 | 11.8 ± 0.8 |
| 363[f] | 0.97 | 2.59 | 0.95 | 4.24−9.11 | 70.7−121 | 16.2 ± 0.9 | 16.3 ± 1.2 | 11.2 ± 0.9 |
| 414[e] | 0.56 | 1.31 | 1.24 | 7.35−17.6 | 112−233 | 32.0 ± 0.6 | 32.2 ± 1.1 | 10.1 ± 0.8 |
| 477[e] | 0.65 | 1.32 | 1.02 | 3.81−15.7 | 69.1−194 | 25.7 ± 0.7 | 26.1 ± 1.4 | 10.4 ± 0.9 |
| 567[e] | 0.76 | 1.29 | 1.10 | 3.14−15.1 | 73.5−177 | 32.8 ± 0.9 | 34.2 ± 2.5 | 10.1 ± 1.1 |
| 663[e] | 0.89 | 1.30 | 0.93 | 3.25−10.9 | 80.5−161 | 35.1 ± 1.6 | 38.1 ± 3.6 | 11.4 ± 1.4 |
| | | | | *trans(cis)*-$CH_3CHCH$[g] | | | | |
| 220 | 0.86 | 3.76 | 2.52 | 5.42−18.2 | 114−220 | 80.0 ± 7.3 | 79.4 ± 6.1 | 7.33 ± 0.93 |
| 243 | 0.95 | 3.78 | 2.50 | 3.59−18.2 | 83.0−186 | 46.4 ± 7.1 | 48.6 ± 4.5 | 7.25 ± 0.81 |
| 266 | 1.04 | 3.77 | 2.44 | 7.06−25.1 | 84.7−196 | 25.3 ± 2.3 | 26.2 ± 5.5 | 6.59 ± 0.75 |
| 266[i] | 0.71 | 2.58 | 2.45 | 7.09−21.4 | 65.0−139 | 11.2 ± 0.9 | 11.4 ± 1.1 | 6.49 ± 0.63 |
| 298 | 0.58 | 1.88 | 1.02 | 7.64−20.5 | 61.5−140 | 19.2 ± 1.8 | 17.1 ± 5.2 | 5.82 ± 0.66 |
| 298 | 1.18 | 3.81 | 4.20 | 6.62−20.2 | 68.1−125 | 11.1 ± 1.1 | 173 ± 6.1 | 5.66 ± 0.80 |
| 298[h,i] | 0.80 | 2.59 | 2.56 | 14.3−47.8 | 143−333 | 51.2 ± 1.8 | 51.7 ± 3.0 | 6.01 ± 0.62 |
| 298[h,i] | 0.81 | 2.62 | 2.46 | 19.7−54.2 | 208−389 | 76.3 ± 2.4 | 77.0 ± 3.3 | 6.16 ± 0.55 |
| 336 | 1.32 | 3.81 | 2.59 | 5.51−19.3 | 40.0−119 | 9.05 ± 2.1 | 9.68 ± 2.0 | 5.55 ± 0.46 |
| 363 | 1.40 | 3.71 | 2.14 | 6.43−21.2 | 39.3−124 | 12.2 ± 1.6 | 12.2 ± 1.7 | 5.03 ± 0.59 |
| 391[h,i] | 1.04 | 2.57 | 2.64 | 17.2−53.2 | 179−360 | 61.3 ± 2.6 | 61.6 ± 2.1 | 5.48 ± 0.53 |
| 458[h,i] | 1.24 | 2.61 | 2.96 | 22.3−79.9 | 230−490 | 85.3 ± 4.2 | 88.6 ± 7.1 | 5.65 ± 0.63 |
| | | | | *cis(trans)*-$CH_3CHCH$[j] | | | | |
| 220 | 0.86 | 3.78 | 1.92 | 5.79−27.3 | 54.6−201 | 30.6 ± 6.8 | 28.2 ± 6.8 | 6.30 ± 0.73 |
| 244 | 0.95 | 3.75 | 1.08 | 3.25−18.7 | 33.8−126 | 15.4 ± 3.3 | 15.4 ± 3.3 | 6.19 ± 0.66 |
| 244 | 1.97 | 7.78 | 1.40 | 4.80−25.6 | 47.2−171 | 19.6 ± 1.0 | 19.7 ± 1.0 | 5.88 ± 0.36 |
| 266 | 1.04 | 3.78 | 2.39 | 4.81−20.0 | 39.6−134 | 16.9 ± 0.8 | 16.8 ± 1.7 | 5.40 ± 0.63 |
| 298 | 1.18 | 3.82 | 2.47 | 7.32−20.3 | 55.8−123 | 12.7 ± 1.6 | 13.7 ± 1.6 | 5.53 ± 0.41 |
| 298[e,i] | 0.79 | 2.56 | 1.95 | 17.5−50.4 | 235−422 | 152 ± 11 | 151 ± 4 | 5.22 ± 0.50 |
| 298[e,i] | 0.40 | 1.30 | 2.74 | 14.7−52.2 | 206−364 | 113 ± 8 | 115 ± 5 | 5.45 ± 0.78 |
| 336 | 1.33 | 3.83 | 3.71 | 5.60−18.4 | 38.0−103 | 14.1 ± 1.9 | 13.0 ± 1.9 | 4.92 ± 0.42 |
| 363 | 1.42 | 3.79 | 5.74 | 6.86−23.6 | 42.7−117 | 13.0 ± 6.1 | 12.5 + 6.1 | 4.59 ± 0.55 |
| 396[e,i] | 1.08 | 2.63 | 2.89 | 13.9−78.6 | 233−481 | 161 ± 13 | 166 ± 8 | 4.61 ± 0.57 |
| 503[e,i] | 1.36 | 2.61 | 3.24 | 24.1−65.2 | 307−527 | 203 ± 16 | 199 ± 5 | 4.83 ± 0.42 |

The shown error for the bimolecular rate coefficients $k$ are $1\sigma$ fitting uncertainties + estimate of other uncertainties. The error limits in $k_{wall}$ are $1\sigma$ fitting uncertainties only. [a]Chlorine lamp with a $CaF_2$ window was used for detection; ArF laser (193 nm), stainless steel with halocarbon wax coated reactor with inner diameter (id) = 1.7 cm, unless otherwise stated. [b]Average of measured wall rates. [c]Wall rate determined from the linear fit $y$-axis intercept. [d]3-Methyl-3-buten-2-one was used as the precursor. [e]Clean quartz reactor with id = 1.7 cm. [f]2-Bromopropene was used as the precursor. [g]*trans*-1-Bromopropene was used as the precursor. [h]Quartz reactor with polydimethylsiloxane (PDMS) coating, id = 1.7 cm. [i]KrF laser (248 nm) was used for photolysis. [j]*cis*-1-Bromopropene was used as the precursor.

coefficients of $CH_3CCH_2$ + $O_2$, *cis*(*trans*)-$CH_3CHCH$ + $O_2$, and *trans*(*cis*)-$CH_3CHCH$ + $O_2$ reactions measured in this work are shown in Figure 4. Also shown are the results of previous measurements of the $CH_3CHCH$ + $O_2$ and $CH_2CH$ + $O_2$ reactions as well as the results of recent calculations of Chen and Goldsmith for the $CH_3CCH_2$ + $O_2$ and *trans*-$CH_3CHCH$ + $O_2$ reactions. As can be seen from Figure 4, the measured bimolecular rate coefficient of reaction 1 has negative temperature dependence up to about 414 K and becomes temperature independent at higher temperatures. Likewise, the bimolecular rate coefficients of reactions 2a and 3a measured in this work behave similarly to reaction 1 and have negative temperature dependence up to about 363 K and become temperature independent at higher temperatures. The thermal stability of the employed precursors limited the upper bound of our experimental temperature range. The Arrhenius expression $k = A \times \exp\left(-\frac{E_a}{RT}\right)$, where $k$ is the bimolecular rate coefficient, $A$ is the pre-exponential factor, $E_a$ is the activation energy, and $R$ is the gas constant, was fitted to the measured bimolecular reaction rate coefficients of reactions 1, 2a, and 3a over the above-mentioned negative temperature dependence range. The following expressions were obtained: $k_1 = (6.51 \pm 0.4) \times 10^{-12} \exp(1.69 \pm 0.14 \text{ kJ mol}^{-1}/RT)$ $cm^3$ $s^{-1}$ ($T$ =



DOI: 10.1021/acs.jpca.8b11017
J. Phys. Chem. A 2019, 123, 999−1006

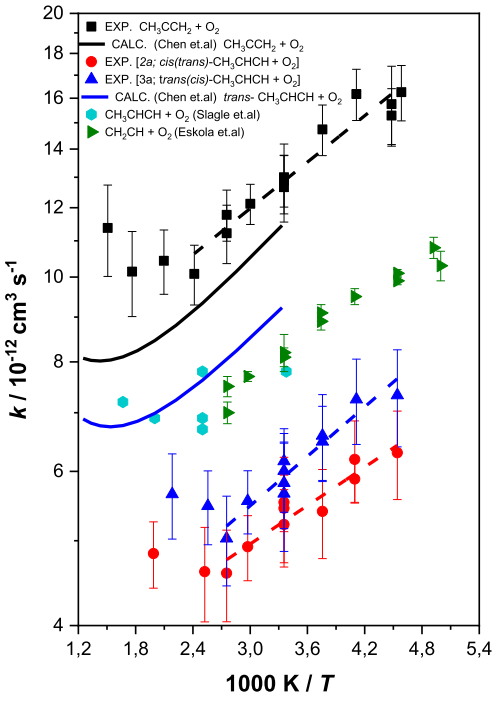


**Figure 4.** Arrhenius plots of the $CH_3CCH_2 + O_2$, *cis*(*trans*)-$CH_3CHCH + O_2$, and *trans*(*cis*)-$CH_3CHCH + O_2$ reactions measured in this work together with previous measurements of the $CH_3CHCH + O_2$ and $CH_2CH + O_2$ reactions, as well as with the results of the recent calculations of Chen and Goldsmith[14] for the $CH_3CCH_2 + O_2$ and *trans*-$CH_3CHCH + O_2$ reactions. Also shown (as dashed lines) are fits of the Arrhenius expression to the negative temperature dependence portions of the current measurements.

218−414 K), $k_{2a} = (2.99 \pm 0.2) \times 10^{-12} \exp(1.40 \pm 0.18 \text{ kJ mol}^{-1}/RT)$ cm$^3$ s$^{-1}$ ($T$ = 220−363 K), and $k_{3a} = (2.86 \pm 0.2) \times 10^{-12} \exp(1.80 \pm 0.18 \text{ kJ mol}^{-1}/RT)$ cm$^3$ s$^{-1}$ ($T$ = 220−363 K). The negative activation energies obtained for reactions 1, 2a, and 3a are close to each other and close to the $E_a = -1.41 \pm 0.18$ kJ mol$^{-1}$ ($T$ = 200−363 K) value Eskola and Timonen[22] obtained for the $CH_2CH + O_2$ reaction.

In Figure 4, our experimental results are compared with the computational results of Chen and Goldsmith.[14] By comparing the temperature dependencies of the $CH_3CCH_2 + O_2$ and *trans*-$CH_3CHCH + O_2$ reactions, one observes that both processes possess similar temperature dependence. In addition, by multiplying the computational results with constant factors [about 1.1 for reaction 1 and about 0.7 for reaction 3a], a good agreement can be obtained over the investigated temperature range. The Chen and Goldsmith[14] results, which are compared in Figure 4, are the total capture rate constants of $CH_3CCH_2 + O_2$ and *trans*-$CH_3CHCH + O_2$ reactions. The similarity of temperature dependencies between experiments and theory may suggest that the negative temperature dependency observed at low temperatures originates from the capture rate, which is an interesting observation.

As discussed in the Experimental Section, $CH_3CHCH$ radical can undergo *cis* ↔ *trans* isomerization with the surplus energy it gains in the photolysis process of the precursor molecule using 193 or 248 nm radiation. In addition, photolysis at 193 nm provides sufficient energy for further isomerization to the allyl radical, see Figure 1. The relative enthalpies of the isomers and their isomerization barriers are shown in Figure 1. However, we observed that the bimolecular rate coefficients of reactions 2a and 3a were independent of photolysis wavelength. This observation shows that any (small) amount of allyl radical possibly produced in measurements using 193 nm photolysis had a negligible effect on kinetic results, because no allyl can be formed in 248 nm photolysis, see Figure 1. Dibble et al.[25] carried out an RRKM/Master Equation analysis of the *trans* ↔ *cis* isomerization of chemically activated 1-methylallyl ($CH_3CHCHCH_2$) radical produced in the OH + *trans*-$CH_3CHCHCH_3$ reaction. The analysis was performed at different levels of initial excitation as a function of total pressure and temperature. Their results suggest that an initial excitation of 5 kcal/mol (21 kJ/mol) or more above the *trans* ↔ *cis* isomerization barrier results in constant *cis*/*trans* population ratio under low-pressure conditions. The calculated *cis*/*trans* population ratio, however, depended on the employed density functional theory method. The results of Dibble et al.[25] may explain why the bimolecular rate coefficients of reactions 2a and 3a measured in this work do not depend on photolysis wavelength employed (193 or 248 nm), although the initial excitation of $CH_3CHCH$ radicals was significantly above the *cis* ↔ *trans* isomerization barrier.

However, we also observed that when the *trans*-$CH_3CHCHBr$ precursor was used to produce the $CH_3CHCH$ radicals, we obtained a slightly but systematically larger rate coefficient for the $CH_3CHCH + O_2$ reaction compared with the rate coefficient obtained when the *cis*-$CH_3CHCHBr$ precursor was used. Because it is very likely that isomerization did take place to some, but unknown extent, the *trans*(*cis*)-$CH_3CHCH + O_2$ and *cis*(*trans*)-$CH_3CHCH + O_2$ notation was employed, as described in the Experimental Section. The current observation that the *trans*(*cis*)-$CH_3CHCH + O_2$ reaction is slightly faster than the *cis*(*trans*)-$CH_3CHCH + O_2$ reaction is in line with the Chen and Goldsmith[14] calculations which show that the potential energy surface (PES) of the *trans*-$CH_3CHCH + O_2$ reaction is slightly more attractive than the PES of the *cis*-$CH_3CHCH + O_2$ reaction. We conclude that the photolysis of the *trans*-$CH_3CHCHBr$ or *cis*-$CH_3CHCHBr$ precursor at 193 or 248 nm results in a mixture of $CH_3CHCH$ isomers for which the initial (nascent) isomer is still in excess after thermalization.

Current results may also be used to interpret the OH + $CH_3CHCH_2$ → *cis*/*trans*-$CH_3CHCH + H_2O$ ($\Delta_r H^{298.15\text{ K}} \approx -35$ kJ/mol) and the subsequent *cis*/*trans*-$CH_3CHCH + O_2$ reaction system. Since the *cis*/*trans*-isomerization barrier is about 18 kJ/mol (see Figure 1) at room temperature, the excitation energy of nascent *cis*/*trans*-$CH_3CHCH$ radical may exceed the barrier by as much as 17 kJ/mol, close to the above-discussed 5 kcal/mol (21 kJ/mol), which in the case of 1-methylallyl, was enough to lead significant isomerization before thermalization. However, in this case the $H_2O$ molecule takes a portion of the 35 kJ/mol energy released in the radical-forming reaction, so that the chemical excitation of the *cis*/*trans*-$CH_3CHCH$ radical is lower than the possible maximum, but might still be more than enough to lead to significant isomerization.

To the best of our knowledge, the kinetic measurements carried out by Slagle et al.[13] employing PIMS is the only study available in the literature regarding the *cis*/*trans*-$CH_3CHCH + O_2$ reaction, and their results are presented in Figure 4. The experimental technique used by Slagle et al.[13] is similar to ours and in the temperature range 296 K−600 K, they observed that the rate coefficient of the *cis*/*trans*-$CH_3CHCH + O_2$ reaction is independent of temperature and bath gas concentration.



DOI: 10.1021/acs.jpca.8b11017
J. Phys. Chem. A 2019, 123, 999−1006

Clearly, this observation is in disparity with our results. We observe explicit negative temperature dependence for the *cis*/*trans*-$CH_3CHCH$ + $O_2$ reactions and the temperature dependence is in good agreement with the computational results of Chen and Goldsmith.[14] Additionally, the bimolecular reaction rate coefficient Slagle et al.[13] measured is on average about 40% faster than those measured in the present work for the *cis*/*trans*-$CH_3CHCH$ + $O_2$ reactions. Such an offset associated with these two apparatuses has already been observed previously.[22,26]

Finally, comparing the bimolecular rate coefficients of reactions 1, 2a, 3a, and $k(CH_2CH + O_2)$[22] shown in Figure 4 manifest that substituting the $\alpha$-H-atom in vinyl radical with a methyl group increases the rate of the reaction by almost 50%, whereas substituting either $\beta$-H-atom of the vinyl radical with a methyl group decreases the rate of reaction by around 30%. The increase of reactivity upon substituting an $\alpha$-H-atom of a radical with a methyl group has been observed many times before[26] but the reduction of reactivity upon substituting a ß-H-atom with a methyl group is a new observation.[27]

## CONCLUSION

In this study, we have measured the bimolecular rate coefficients of the $CH_3CCH_2$ + $O_2$ and *cis*/*trans*-$CH_3CHCH$ + $O_2$ reactions over wide temperature ranges at low pressures. The bimolecular rate coefficients of all the three reactions were found to have a negative temperature dependence at temperatures below about 380 K and appear to become independent of temperature at somewhat higher temperatures, in good agreement with the recent computational study of Chen and Goldsmith.[14] On the other hand, current results show that the $CH_3CCH_2$ + $O_2$ reaction is faster and *trans*-$CH_3CHCH$ + $O_2$ reaction slower than their computational study suggests. As expected, no bath gas concentration dependence was observed for any of the reactions studied in the employed pressure range (0.3−1.5 Torr). The observed products of $CH_3CCH_2$ + $O_2$ and *cis*/*trans*-$CH_3CHCH$ + $O_2$ reactions show that their reaction mechanism is analogous to the reaction of vinyl radicals with molecular oxygen.

## ASSOCIATED CONTENT

### Supporting Information

The Supporting Information is available free of charge on the ACS Publications website at DOI: 10.1021/acs.jpca.8b11017.

Supplementary Figure S1 and the details of electronic structure calculations (PDF)

## AUTHOR INFORMATION


### Corresponding Author

*E-mail: arkke.eskola@helsinki.fi.

### ORCID

Arkke J. Eskola: 0000-0002-2249-2726


### Notes

The authors declare no competing financial interest.

## ACKNOWLEDGMENTS

S.P.J. and A.J.E. acknowledge support from the Academy of Finland, Grant Nos. 294042/319353, 311967, and 288377. T.T.P. acknowledges support from the Doctoral Programme in Chemistry and Molecular Sciences of the University of Helsinki. The work of G.L. was supported by the National Research, Development and Innovation Agency (Grant No. K129140) and by the Government of Hungary, cofinanced by the European Regional Development Fund under the project VEKOP-2.3.2-16-2017-00013. The authors thank Prof. C.F. Goldsmith for helpful discussions and providing calculated total rate coefficients of $CH_3CCH_2$ + $O_2$ and *trans*-$CH_3CHCH$ + $O_2$ reactions.

## REFERENCES


(1) Wilk, R. D.; Cernansky, N. P.; Pitz, W. J.; Westbrook, C. K. Propene Oxidation at Low and Intermediate Temperatures: A Detailed Chemical Kinetic Study. *Combust. Flame* **1989**, *77*, 145−170.

(2) Morganti, K. J.; Foong, T. M.; Brear, M. J.; da Silva, G.; Yang, Y.; Dryer, F. L. The Research and Motor Octane numbers of Liquefied Petroleum Gas (LPG). *Fuel* **2013**, *108*, 797−811.

(3) Mohamed, S. Y.; Cai, L.; Khaled, F.; Banyon, C.; Wang, Z.; Al Rashidi, M. J.; Pitsch, H.; Curran, H. J.; Farooq, A.; Sarathy, S. M. Modeling Ignition of a Heptane Isomer: Improved Thermodynamics, Reaction Pathways, Kinetics, and Rate Rule Optimizations for 2-Methylhexane. *J. Phys. Chem. A* **2016**, *120*, 2201−2217.

(4) Dryer, F. L.; Brezinsky, K. A. Flow Reactor Study of the Oxidation of n-Octane and Iso-Octane. *Combust. Sci. Technol.* **1986**, *45*, 199−212.

(5) Burke, S. M.; Burke, U.; Mc Donagh, R.; Mathieu, O.; Osorio, I.; Keesee, C.; Morones, A.; Petersen, E. L.; Wang, W.; DeVerter, T. A.; et al. An Experimental and Modeling Study of Propene Oxidation. Part 2: Ignition Delay Time and Flame Speed Measurements. *Combust. Flame* **2015**, *162*, 296−314.

(6) Moldoveanu, S. C. *Pyrolysis of Organic Molecules: Applications to Health and Environmental Issues*; Elsevier: 2009; Vol. *28*.

(7) Law, C. K. *Combustion Physics*; Cambridge University Press: 2010.

(8) Glassman, I.; Yetter, R. A.; Glumac, N. G. *Combustion*; Academic Press: 2014.

(9) Ruscic, B.; Pinzon, R. E.; Morton, M. L.; von Laszevski, G.; Bittner, S. J.; Nijsure, S. G.; Amin, K. A.; Minkoff, M.; Wagner, A. F. Introduction to Active Thermochemical Tables: Several Key Enthalpies of Formation Revisited. *J. Phys. Chem. A* **2004**, *108*, 9979−9997.

(10) Ruscic, B.; Pinzon, R. E.; Von Laszewski, G.; Kodeboyina, D.; Burcat, A.; Leahy, D.; Montoy, D.; Wagner, A. F. Active Thermochemical Tables: Thermochemistry for the 21st Century. *J. Phys.: Conf. Ser.* **2005**, *16*, 561.

(11) *ATcT: Active Thermochemical Tables*, version 1.122; Argonne National Laboratory: 2016; http://atct.anl.gov.

(12) Burke, S. M.; Metcalfe, W.; Herbinet, O.; Battin-Leclerc, F.; Haas, F. M.; Santner, J.; Dryer, F. L.; Curran, H. J. An Experimental and Modeling Study of Propene Oxidation. Part 1: Speciation Measurements in Jet-Stirred and Flow Reactors. *Combust. Flame* **2014**, *161*, 2765−2784.

(13) Slagle, I. R.; Bernhardt, J. R.; Gutman, D. Kinetics of the Reactions of Unsaturated Free Radicals (Methylvinyl and *i*-$C_4H_3$) With Molecular Oxygen. *Symp. (Int.) Combust., [Proc.]* **1989**, *22*, 953−962.

(14) Chen, X.; Goldsmith, C. F. A Theoretical and Computational Analysis of the Methyl-Vinyl + $O_2$ Reaction and Its Effects on Propene Combustion. *J. Phys. Chem. A* **2017**, *121*, 9173−9184.

(15) Yang, R.; Yu, L.; Jin, X.; Zhou, M.; Carpenter, B. K. Reaction of Vinyl Radical With Oxygen: A Matrix Isolation Infrared Spectroscopic and Theoretical Study. *J. Chem. Phys.* **2005**, *122*, 014511.

(16) Westmoreland, P. R. Thermochemistry and Kinetics of $C_2H_3$ + $O_2$ Reactions. *Combust. Sci. Technol.* **1992**, *82*, 151−168.

(17) Wang, H.; Wang, B.; He, Y.; Kong, F. The Gaseous Reaction of Vinyl Radical With Oxygen. *J. Chem. Phys.* **2001**, *115*, 1742−1746.

(18) Slagle, I. R.; Park, J. Y.; Heaven, M. C.; Gutman, D. Kinetics of Polyatomic Free Radicals Produced by Laser Photolysis. 3. Reaction of Vinyl Radicals With Molecular Oxygen. *J. Am. Chem. Soc.* **1984**, *106*, 4356−4361.




DOI: 10.1021/acs.jpca.8b11017
*J. Phys. Chem. A* 2019, 123, 999−1006

(19) Park, J.-Y.; Heaven, M. C.; Gutman, D. Kinetics and Mechanism of the Reaction of Vinyl Radicals With Molecular Oxygen. *Chem. Phys. Lett.* **1984**, *104*, 469−474.
(20) Mebel, A. M.; Kislov, V. V. The $C_2H_3 + O_2$ Reaction Revisited: Is Multireference Treatment of the Wave Function Really Critical? *J. Phys. Chem. A* **2005**, *109*, 6993−6997.
(21) Feng, W.; Wang, B. Reaction of Vinyl Radical With $O_2$ Studied by Time-Resolved Infrared Emission Spectroscopy. *Chem. Phys. Lett.* **2002**, *356*, 505−510.
(22) Eskola, A. J.; Timonen, R. S. Kinetics of the Reactions of Vinyl Radicals With Molecular Oxygen and Chlorine at Temperatures 200−362 K. *Phys. Chem. Chem. Phys.* **2003**, *5*, 2557−2561.
(23) Luo, Y.-R. *Handbook of Bond Dissociation Energies in Organic Compounds*; CRC Press: 2002.
(24) Bencsura, A.; Knyazev, V. D.; Slagle, I. R.; Gutman, D.; Tsang, W. Weak Collision Effects in the Reaction $CH_3CO \leftrightarrow CH_3 + CO$. *Ber. Bunsen-Ges. Phys. Chem. Chem. Phys.* **1992**, *96*, 1338−1347.
(25) Dibble, T. S.; Sha, Y.; Thornton, W. F.; Zhang, F. Cis−Trans Isomerization of Chemically Activated 1-Methylallyl Radical and Fate of the Resulting 2-Buten-1-Peroxy Radical. *J. Phys. Chem. A* **2012**, *116*, 7603−7614.
(26) Pekkanen, T. T.; Arppe, S. L.; Eskola, A. J.; Rissanen, M. P.; Timonen, R. S. An Experimental Study of the Kinetics of the Reactions of Isopropyl, sec-Butyl, and tert-Butyl Radicals with Molecular Chlorine at Low Pressures (0.5−7.0 Torr) in the Temperature Range 190−480 K. *Int. J. Chem. Kinet.* **2016**, *48*, 796−805.
(27) Eskola, A. J.; Lozovsky, V. A.; Timonen, R. S. Kinetics of the Reactions of $C_2H_5$, n-$C_3H_7$, and n-$C_4H_9$ Radicals with $Cl_2$ at the Temperature Range 190−360 K. *Int. J. Chem. Kinet.* **2007**, *39*, 614−619.



DOI: 10.1021/acs.jpca.8b11017
*J. Phys. Chem. A* 2019, 123, 999−1006